

# Temperature-programmed desorption analysis for aminofunctionalized zeolite nanomaterials

Saeed S. Ba Hashwan<sup>1</sup>, Mohd Haris Md Khir<sup>1</sup>, Illani Mohd Nawi<sup>1</sup>, Muzamil A. Hassan<sup>2</sup>, Abdullah S. Algamili<sup>3</sup>, Hussein Shutari<sup>3,\*</sup>

<sup>1</sup>Department of Electrical and Electronic Engineering, Universiti Teknologi PETRONAS, Bandar Seri Iskandar, 32610, Perak, Malaysia

<sup>2</sup>Chemical Engineering Department College of Engineering and Technology, University of Doha for Science and Technology (UDST), Doha, Qatar

<sup>3</sup>School of Electrical and Electronic Engineering, Universiti Sains Malaysia, Nibong Tebal, 14300, Penang, Malaysia

\*) Email: shutari2000@outlook.com

Received 11/5/2025, Received in revised form 23/8/2025, Accepted 9/9/2025, Published 15/10/2025

In this study, Zeolite nanomaterial has been functionalized with amino functional groups using APTES (3-aminopropyltriethoxysilane) solution with 20%, 40%, 60% and 80% wt. The prepared amine zeolite has been investigated for its ability to adsorb carbon dioxide gas molecules using Temperature-Programmed Desorption (TPD). Furthermore, the results of the TPD characterization show that zeolite with 60%wt APTES has a high adsorption capacity of CO<sub>2</sub> with more than 4000 µmole/g compared with other APTES concentration where the 60%wt improved the adsorption capacity four-fold. The effective improvement in CO<sub>2</sub> adsorption performance by amine-modified zeolite is attributed to the APTES modification reaction, which introduces additional functional groups onto the zeolite surface, thus, increasing the number of active sites available for CO<sub>2</sub> adsorption. The TDP results show that zeolite is a promising material for CO<sub>2</sub> adsorption. Additionally, the zeolite functionalized with 60% amino functional groups is characterized by FTIR, XRD, FESEM, EDX, XPS, and TGA.

**Keywords:** Temperature-Programmed Desorption; Zeolite; Adsorption; CO<sub>2</sub>.

### 1. INTRODUCTION

Zeolites are crystalline aluminosilicate materials characterized by well-defined pores and channels, commonly used in catalysis and adsorption applications [1], often used in various industrial applications such as sensing [2], catalysis [3], gas storage [4], gas separation [5], as well as energy storage [6]. Therefore, zeolite has attracted significant attention in various scientific disciplines due to their tunable structures, large surface area, high porosity, facile synthetic strategies, stability, and catalytic nature [7].

Additionally, because of the spread of dangerous gases in the environment resulting from the emergence of new industries over the past 10 years, there has been considerable growth in CO<sub>2</sub> adsorption and utilization [8]. These applications may contribute to improving the environment by detecting these dangerous gases and improving the process of eliminating them, thereby preserving our health and safety [9]. More than 70% of the global energy is reportedly to be supplied by fossil fuel stations, which are responsible for the production of carbon dioxide [10]. Various gases are released into the environment; however, the CO<sub>2</sub> gas is the main cause of the greenhouse and climate change that the world is facing today [11]. Therefore, the development of materials which are capable of CO<sub>2</sub> adsorption has been attracting significant attention to adsorb the amount of gas released from all types of automobile engines, refineries, and even gas turbines [12].

Mfoumou et al. [13] have performed a study to investigates physiosorbed and chemisorbed CO<sub>2</sub> species on NaX zeolite and its cation-exchanged forms, using temperature programmed desorption (TPD) and infrared (IR) spectroscopy. they found that the cationic modification of NaX zeolite slightly enhances CO<sub>2</sub> physisorption and significantly strengthens CO<sub>2</sub> chemisorption, favoring the formation of more stable carbonate species. In addition, Suba et al. [14] have investigated the adsorption-desorption of zeolite with APTES amino functionalized for carbon dioxide. They found that the adsorption-desorption behavior of the APTES-amino functionalized zeolite is consistent with the adsorption capacity of the APTES even after nine consecutive cycles. The composites are synthesized with three different concentrations of APTES: 20, 30, and 40 wt.%.

Furthermore, Shezad et al. [15] have developed a robust nickel-based catalyst supported on hierarchical zeolite 13X (h13X) for the efficient methanation of carbon dioxide (CO<sub>2</sub>). The catalyst design involved the surface functionalization of h13X using (3 aminopropyl) triethoxysilane (APTES) to enhance metal-support interaction (MSI) and facilitate the uniform dispersion of Ni nanolayers with thicknesses ranging from 1.5 to 7 nm. Characterization techniques including scanning transmission electron microscopy (STEM) and X-ray photoelectron spectroscopy (XPS) confirmed the successful deposition of Ni and a significant shift in binding energies, indicative of 2 improved MSI. Temperature-programmed reduction (H2-TPR) and CO<sub>2</sub> temperature programmed desorption (CO<sub>2</sub>-TPD) analyses demonstrated the influence of APTES grafting and reaction temperature on the reducibility and surface basicity of the catalysts. Under optimized conditions, the catalyst achieved a CO<sub>2</sub> conversion of 61% and a high CH4 selectivity of 97%, maintaining stable activity over 150 hours without noticeable deactivation. These results underscore the significance of surface chemical modification of the support in enhancing catalyst performance and stability for CO<sub>2</sub> hydrogenation applications [15].

Therefore, in this work, zeolite nanomaterial has been developed to be used as an adsorption material for CO<sub>2</sub>. Zeolites are considerably more affordable and produced in greater quantities for industrial applications compared with silicate materials. Zeolite is modified with different concentrations of amine groups using APTES and examined using TPD characterization to investigate the capability of the zeolite for CO<sub>2</sub> adsorption. This study also shows the prepared zeolite characters obtained by various characterization techniques such as FTIR, XRD, FESEM, EDX, XPS, and TGA.

### 2. EXPERIMENTAL

#### 2.1 Materials

Zeolite powder and (3-Aminopropyl) triethoxysilane (APTES, 98% purity) are procured from Sigma-Aldrich, Toluene, which served as the organic solvent for the functionalization process, is obtained from Merck (Germany). All reagents are used as received, without undergoing any additional purification, to preserve their original chemical properties and ensure consistency across experiments. Throughout all stages of material preparation and sample modification, deionized (DI) water is utilized to eliminate the potential influence of ionic contaminants that may arise from tap or distilled water. The use of high-purity solvents and reagents, along with DI water, ensures the reliability and reproducibility of the functionalization and characterization processes.

# 2.2 Preparation of zeolite modified by APTES

APTES-modified zeolite is prepared using the impregnation method by which the desired amount of APTES solutions is dissolved in 15 ml of toluene solvent [16]. In more detail, solutions with different concentrations of APTES corresponding to 20%wt, 40%wt, 60%wt, and 80%wt loaded with respect to zeolite powder are prepared in toluene solvent. The desired number of APTES is mixed in 15 ml of toluene solvent and stirred for 10 minutes before adding (1 g) of zeolite followed by an ultrasonic process for 2 hours. Figure 1 (a) illustrates the zeolite preparation process. The prepared solutions are left to settle for 5 hours in the fume hood at room temperature, this is to allow the solvent to evaporate, followed by heat treatment at 100 °C for 12 hours. Figure 2 presents the morphology of the zeolite sample that has been synthesized and subsequently functionalized using (3-Aminopropyl) triethoxysilane (APTES). The modification of the surface with APTES introduces amine functional groups to the zeolite framework, which are known to enhance interactions with acidic gases such as carbon dioxide Co<sub>2</sub> through chemisorption and hydrogen bonding mechanisms. This modification aims to improve the selectivity and adsorption capacity of the zeolite toward CO<sub>2</sub> capture applications. To evaluate the CO<sub>2</sub> adsorption performance of these APTES-functionalized zeolite materials, Temperature Programmed Desorption (TPD) analysis will be conducted. In this technique, the sample is first exposed to CO<sub>2</sub> gas, allowing adsorption to occur. Subsequently, the temperature is gradually increased under an inert gas atmosphere, and the desorbed CO<sub>2</sub> is measured as a function of temperature. This provides critical insights into the strength and nature of the interaction between the CO<sub>2</sub> molecules and the modified surface. Through TPD, it is possible to determine key parameters such as the desorption temperature, adsorption capacity, and the binding energy of the adsorbed CO<sub>2</sub> species. These data help in assessing the efficiency of the modified zeolites as CO<sub>2</sub> adsorbents and in identifying the optimal operating conditions for potential gas separation or environmental remediation applications.



Figure 1 Schematic illustrations for Zeolite sensing material development.

#### 2.3 Characterization

The TPDRO process is performed using a Thermo Scientific machine (TPDRO 1110). Furthermore, the FTIR technique has been used to investigate and verify the presence of the functional groups on the surface of the zeolite material by using FTIR (Perkin Elmer). FTIR analysis is done using the KBr pellets containing zeolite powder and experiment is performed in the range of 400 to 4000 cm<sup>-1</sup>. Additionally, XRD experiment is performed using a Panalytical X'pert Powder machine with a scan range of  $2\theta$  and from 2 to  $80^{\circ}$ , with  $CuK\alpha$  1.54 °A radiation. All the samples are in powder with approximately amount of 200 mg for each sample.

The surface morphology of the unmodified and modified zeolite with APTES has been observed using Field-Emission Scanning Electron Microscope (FESEM)-Energy Dispersive X-Ray (Model: Zeiss Supra 55 VP) at 5.00 Kv and at 1-30 kx magnification. As well as the modified zeolite with 60% APTES is inspected by using TEM. TEM inspection is performed using the Hitachi HT7800 Series, where a small amount of powder zeolite sample is dispersed in ethanol solvent followed by sonication for 15 minutes, and kept it standing for five minutes. Then two to three drops of the solution are dropped into the TEM Cu grid and dried, followed by the TEM inspection. Thermogravimetric Analysis (TGA) and X-ray Photoelectron Spectroscopy (XPS) are performed to evaluate the thermal stability, surface composition, and chemical bonding states of the unmodified and modified zeolite samples.

For the TGA analysis, both unmodified zeolite and zeolite functionalized with 60% (3-Aminopropyl) triethoxysilane (APTES) are examined using a Perkin Elmer Simultaneous Thermal Analyzer (STA) 6000. This technique is employed to monitor weight changes as a function of temperature under a controlled heating program. The primary objective is to assess the thermal stability of the materials, determine the onset and extent of decomposition, and quantify the proportion of volatile components, such as moisture, residual solvents, and organic functional groups introduced through surface modification. In TGA, three fundamental parameters—temperature, mass, and time—are continuously recorded. From these measurements, additional insights such as degradation onset temperature, rate of weight loss, and total decomposition percentage are obtained. The mass measurement is performed

## Exp. Theo. NANOTECHNOLOGY 9 (2025) 539-553

continuously as the sample temperature increases, enabling the identification of distinct thermal events, including dehydration, desorption of physically adsorbed species, and decomposition of chemically bonded moieties. This analysis is critical for understanding the robustness of the zeolite structure and the stability of the grafted functional groups.

XPS analysis is conducted using a Thermo Scientific K-Alpha spectrometer, with Avantage 4.45 software for spectral acquisition and processing. The modified zeolite is tested in powder form to investigate the surface elemental composition and the chemical states of the detected elements. The sample powder is evenly spread onto the sample platter to ensure representative measurement, then mounted into the sample holder and introduced into the loading chamber. After reaching the required high-vacuum conditions, the sample is transferred into the analysis chamber, where it is irradiated with a focused X-ray beam to induce photoelectron emission from the surface atoms. The resulting spectra, representing the binding energies of the emitted electrons, are recorded and subsequently processed using Avantage 4.45 software. This analysis enables precise identification of elemental peaks, quantification of elemental composition, and determination of the chemical bonding environment, thereby confirming the successful incorporation of functional groups on the zeolite surface.

#### 3. RESULTS AND DISCUSSION

# 3.1 The prepared zeolite

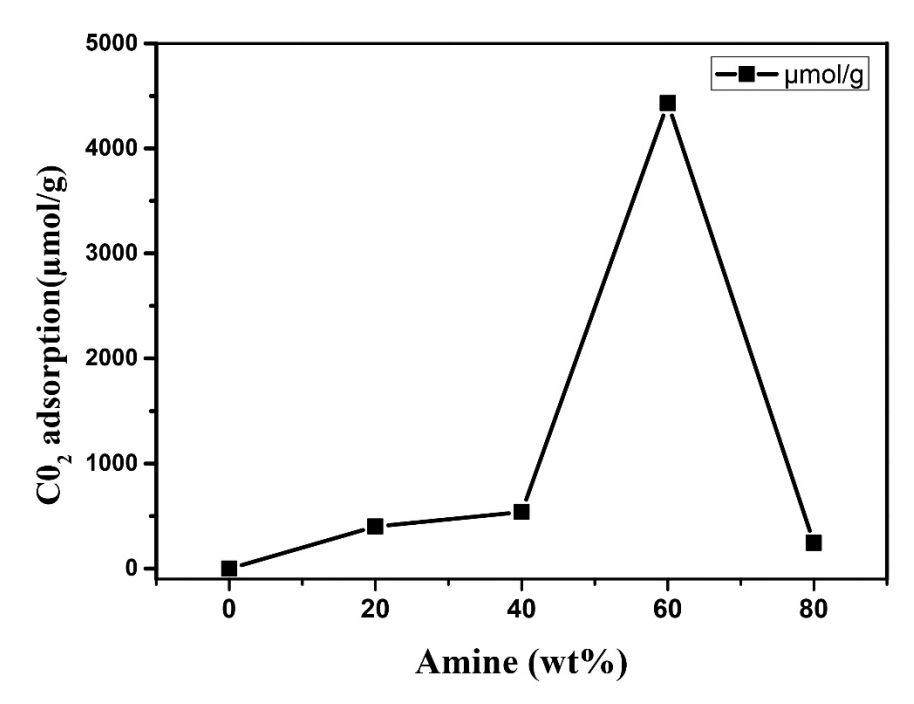
The zeolite material has been functionalized using Amino functional groups using amino-propyltriethoxysilane (APTES) with four different concentrations 20%, 40%, 60% and 80% wt. Then, the CO<sub>2</sub> temperature-programmed desorption (TPD) studies are carried out using a fixed flow system [34]. In the experiment, the samples prepared are exposed to CO<sub>2</sub>, and the adsorption amount of CO<sub>2</sub> by the different samples is recorded as presented in Figure 3. The 60% modified zeolite is presented with the highest adsorption capacity by around 4000 μmole/g of CO<sub>2</sub>. Therefore, 60% wt. of modified zeolite has been considered the best choice to be used as an adsorption layer [17].



Figure 2 Schematic illustrations for Zeolite sensing material development.

## 3.2 Temperature-programmed desorption study

The TPDRO process is performed using the machine with Model: Thermo Scientific (TPDRO 1110). The CO<sub>2</sub> TPD studies are carried out using a fixed-bed flow system. Around 100 mg of unmodified and modified zeolite materials are used in the experiment as sorbent materials and are placed in a quartz tubular reactor. Nitrogen at a flow rate of 20 cm<sup>3</sup> min<sup>-1</sup> is passed through the reactor at room temperature followed by Helium gas passing through with an increase in the temperature at a rate of 40 °C min<sup>-1</sup> to 200 °C and it is kept at 200 °C for 10 minutes before return to the room temperate. This process is carried out to remove the moisture and any other volatile molecules on the samples [18]. Then the CO<sub>2</sub> gas is introduced into the chamber and passed through the sorbent sample at a flow rate of 20 cm<sup>3</sup> min<sup>-1</sup> with temperature ramp up at a rate of 40 °C min<sup>-1</sup> to 75 °C and the gas is left flow over the sample for a further 30 minutes to ensure full saturation of the CO<sub>2</sub> and the reactor is under continuous observation using the mass spectroscopy [13,19].



**Figure 3** Temperature programmed desorption study for the zeolite modified by Amine APTES with increasing wt.% Amine capacities of CO<sub>2</sub> adsorption.

## 3.3 FTIR analysis

FTIR spectra is obtained to investigate the effect of the functionalization process, with a comparative analysis performed between the raw and modified zeolite materials. As shown in Figure 4, the transmittance spectra reveals that the main structural framework of zeolite remains intact after surface modification, confirming that the functionalization process does not compromise the integrity of the material's chemical or molecular structure [20]. In the low wavenumber region (653–1014 cm<sup>-1</sup>), both samples exhibit characteristic bands corresponding to the internal vibrations of the zeolite framework, such as Si–O–Si and Si–O–Al stretching, indicating the preservation of the crystalline structure. Notably, the broad absorption band observed around 3440 cm<sup>-1</sup> corresponds to the O–H stretching vibrations, which is associated with surface hydroxyl (–OH) and carboxyl (–COOH) groups. The presence of these functional groups, especially the carboxyl group, is significant for enhancing the material's ability to interact with carbon dioxide molecules through hydrogen bonding and acid–base interactions [16, 21]. Furthermore, the appearance of C–H stretching vibrations near 2942 cm<sup>-1</sup> in the modified zeolite

confirms the successful grafting of organic moieties, such as aminopropyl groups from APTES, onto the zeolite surface. These changes collectively indicate that functionalization has been effectively achieved, improving the material's chemical functionality without altering its core framework.

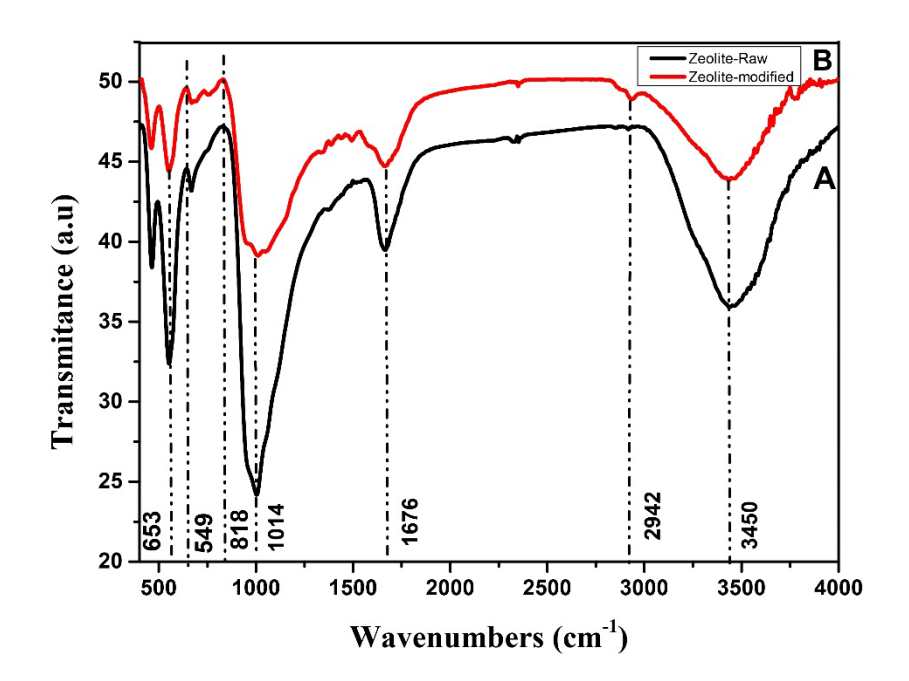


Figure 4 FTIR spectra of Raw Zeolite (A), and 60% wt. Modified Zeolite (B).

# 3.4 XRD analysis

The XRD patterns of the unmodified and the prepared zeolite are presented in Figure 5. The zeolite nanomaterial is composed of two different elements to form the composite, which are the  $SiO_2$  and  $Al_2O_3$ . From the XRD pattern in Figure 5, the major phases for the composite are observed, with the most intense peak at around  $26.57^{\circ}2\theta$  and  $30^{\circ}2\theta$ . The obtained XRD pattern has been investigated with literature where several techniques are employed to identify the material structure. It is evidenced that the obtained pattern corresponds to a cubic crystalline structure, indicating the space group and lattice parameters characteristic of zeolite a=b=c=24.61 °A [22–24]. Additionally, the Scherrer's formula is used to measure the crystallite size of the zeolite. Based on the XRD pattern, the structural properties extracted are summarized in the table below [25].

<b>2θ</b> (°)	Miller Indices (hkl)	d-spacing (nm)	FWHM (rad)	Cos (0)	Crystallite Size (nm)
6.2	(111)	1.425	0.0204	0.997	11.88
10.0	(220)	0.884	0.0303	0.992	9.30
15.5	(311)	0.571	0.0405	0.985	8.09
23.5	(440)	0.378	0.0452	0.970	7.24
29.4	(533)	0.304	0.0526	0.957	6.14
34.9	(555)	0.257	0.0582	0.944	6.29

**Table 1** Structural parameters extracted from XRD pattern.

Table 1 presents the structural parameters of the synthesized zeolite material, which are extracted from the XRD pattern using Scherrer's equation. The analysis is limited to diffraction peaks observed below 35° (2θ), which correspond to the most intense and structurally relevant reflections in low-angle zeolite structures. The peaks are assigned to typical Miller indices (hkl) commonly found in faujasite-type zeolites (e.g., NaX or NaY). The 2θ values ranged from 6.2° to 34.9°, corresponding to reflections such as (111), (220), (311), (440), and (555). These orientations confirm the crystalline nature and phase purity of the material, aligning well with standard zeolite XRD profiles [26]. Crystallite sizes, which are calculated by using Scherrer's formula, range from approximately 6.14 nm to 11.88 nm. The largest crystallites are found at the lowest angle peak (6.2° 2θ), which is typical since lower angle peaks generally represent larger interplanar spacing and lower strain broadening. As the angle increases, the calculated crystallite size decreases slightly, likely due to increasing peak broadening and microstructural effects [27]. These values indicate that the synthesized zeolite is nanocrystalline in nature, with relatively uniform crystallite dimensions. Such nanoscale crystal sizes are desirable in gas adsorption and catalytic applications due to increased surface area and accessible active sites [28].

$$D = \frac{\kappa\lambda}{\beta\cos\theta} \tag{1}$$

where D is crystallite size (in nanometers, nm), K is shape factor, typically 0.9,  $\lambda$  is X-ray wavelength (Cu K $\alpha$  = 0.15406 nm),  $\beta$  is Full Width at Half Maximum (FWHM) in radians, and  $\theta$  is Bragg angle (half of 2 $\theta$ ).

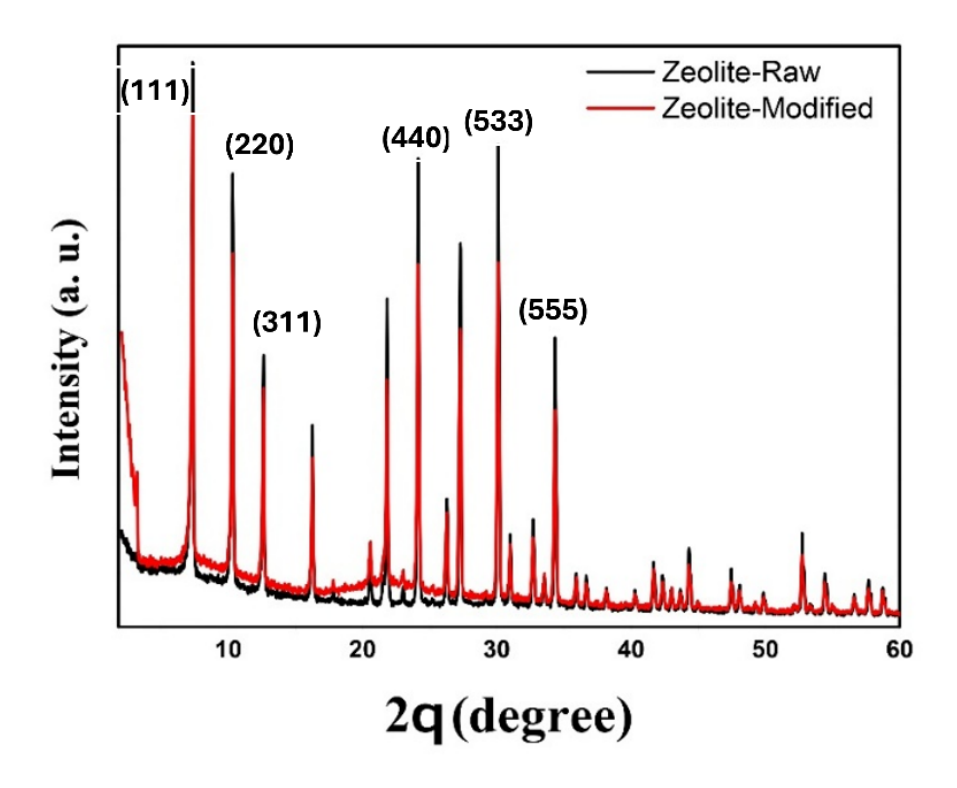


Figure 5 XRD patterns of Raw Zeolite (A), and Modified Zeolite (B).

## 3.5 FESEM analysis

The prepared zeolite sensing layer has been characterized by using FESEM to investigate the surface morphology, as shown in Figure 6. The zeolite surface is found to be cubic with an extremely small size, which provides a high surface area [29, 30]. This high surface area is significantly important in the reaction which provides enough molecules to react with the desired gas molecules. Figure 6 (d) presents the 30 kx magnification which has demonstrated the structure of the zeolite clearly. Field Emission Scanning Electron Microscopy (FESEM) is conducted to evaluate the surface morphology and grain size of the synthesized zeolite material. The micrographs reveal that the particles exhibit a relatively uniform morphology with slight agglomeration.

The grains appear in a near-spherical or polyhedral form, which is typical of synthesized zeolites prepared via hydrothermal methods. The average grain size observed from FESEM images is estimated to be in the range of 60–80 nm. This size represents the physical dimensions of aggregated particles or grains, which may consist of multiple smaller crystallites. This observation supports the inference drawn from the XRD analysis, where the crystallite sizes calculated using Scherrer's equation ranged between 6.14 nm and 11.88 nm.

The discrepancy between the XRD and FESEM measurements is expected, as XRD determines the size of coherently diffracting domains (crystallites), while FESEM visualizes the overall particle morphology, including possible crystallite clusters, agglomerates, or polycrystalline grains. These results confirm that the synthesized zeolite is nanostructured, with the crystallite sizes contributing to high surface area and the grain size confirming the physical uniformity of the material. This nanoscale architecture is advantageous for applications involving adsorption, ion exchange, and catalysis, where both high surface area and accessible porosity are essential.

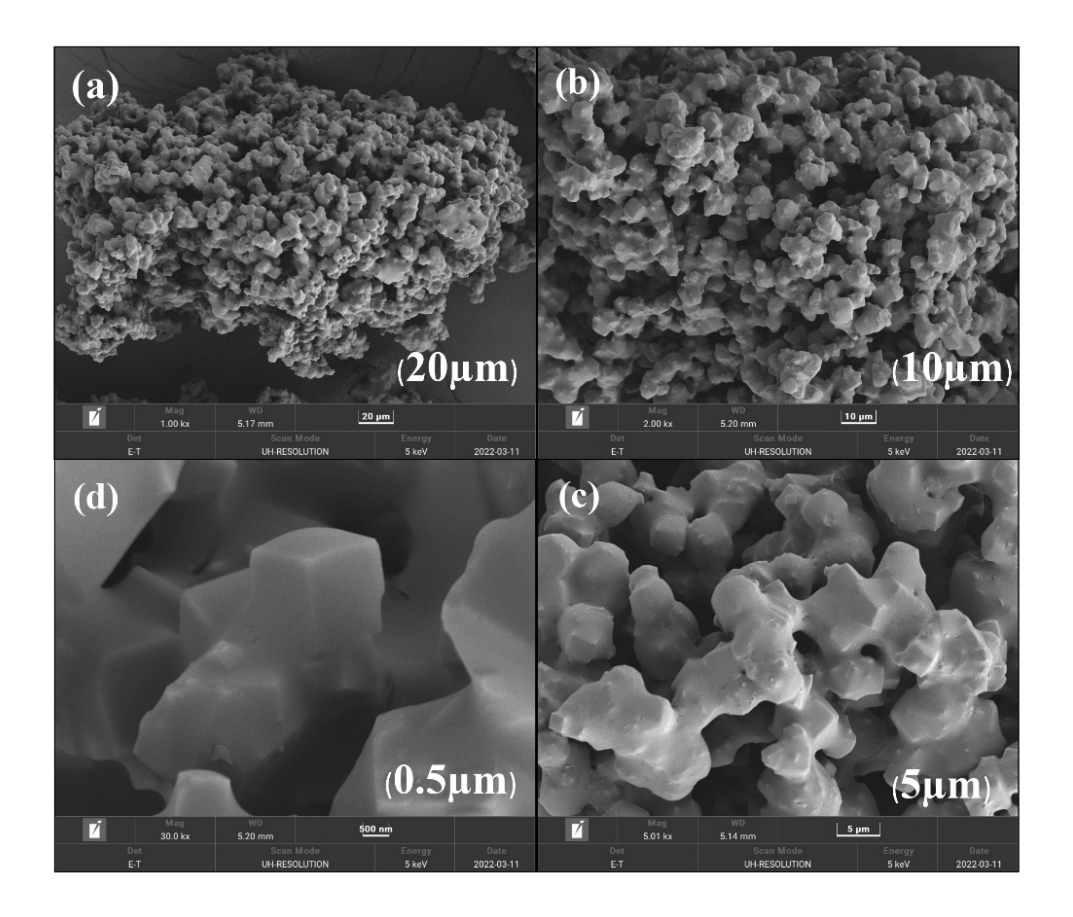


**Figure 6** Typical zeolite structure presents by FESEM (A) Zeolite with the 1.00 kx magnification, (B) Zeolite with the 2.00 kx magnification, (C) Zeolite with the 5.00 kx magnification and (C) Zeolite with the 30.00 kx magnification.

### 3.6 EDX characterization for zeolite

Energy dispersive X-ray spectroscopy (EDX) is done to study the chemical composition of zeolite. The EDX spectrum of the zeolite is observed by the EDX Oxford instrument. The EDX analysis of the modified zeolite sample can provide information about the types and amounts of elements present in the material, including the main framework elements (such as aluminum, silicon, and oxygen) as well as any additional elements present in the structure or adsorbed on the surface. In EDX analysis, the zeolite sample is bombarded with a beam of high-energy electrons, which causes the zeolite to emit characteristic X-rays. These X-rays are then detected and analyzed to determine the elemental composition of the sample [31]. The zeolite framework sample presents the elements, including Si, Al, O, Na, and C in the EDX as shown in Figure 7.

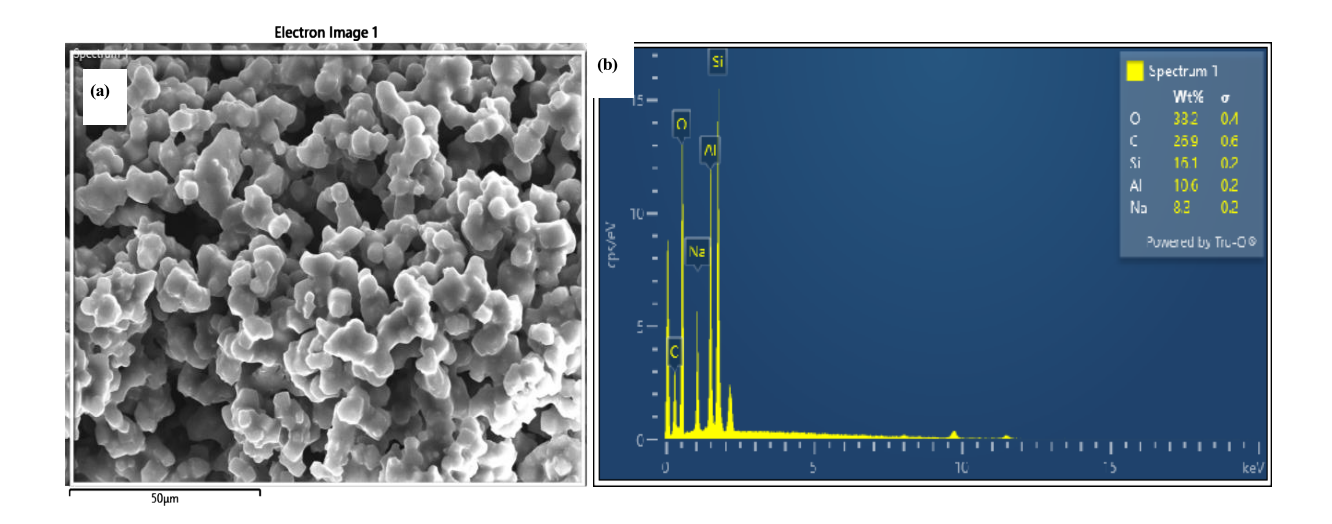


**Figure 7** Energy dispersive X-ray spectroscopy for the modified zeolite.

# 3.7 XPS analysis

The XPS analysis provides an analysis of zeolite surface chemistry, which is important for understanding their properties and performance. The XPS can also provide information about the elemental composition and chemical state of the top few nanometers of a sample. In addition, zeolites are crystalline aluminosilicate materials with regular microporous structures. Figure 8 shows the peaks for the zeoilte, which is composed of silca and aluminum. Furthermore, the modified zeolite presents the formation of carboxylic groups, which is important for zeolite applications [32]. Figure 8 shows the XPS spectrum of zeolite, and the peaks for possible elements such as Al 2p, Si 2p, and O 1s are observed at binding energies of 74, 102.8, and 532 eV, respectively [33].

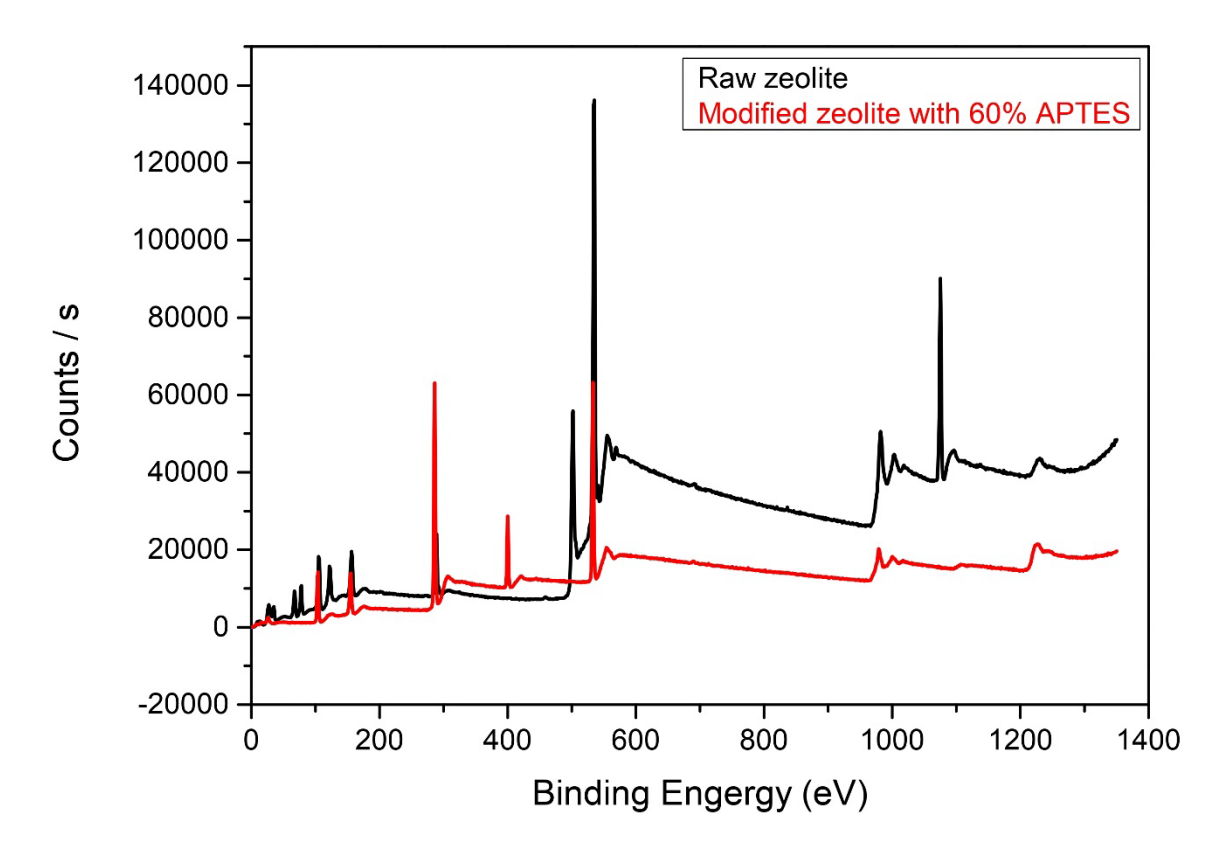


**Figure 8** XPS for the raw and the modified zeolite with 60 % APTES.

## 3.7 TGA analysis

TGA analysis is a technique used to study the thermal behavior of the zeolite sensing layer as it is heated to identify the burn temperature of the material. Furthermore, during TGA analysis, the zeolite samples have been heated at a constant rate while their weight is continuously monitored. The weight changes occur as the temperature increases give information about the thermal stability and composition of zeolite material. The TGA curve, as shown in Figure 9 for the unmodified and modified zeolite sensing materials, typically shows a weight loss due to the release of adsorbed water molecules from the pores of the zeolite structure at a temperature of 200 °C. This is known as the zeolite's dehydration behavior, and the temperature at which the weight loss occurs is referred to as the zeolite's dehydration temperature. The TGA curve also reveals any other weight loss that may occur due to thermal decomposition, oxidation, or other chemical reactions involving the zeolite material. Therefore, the unmodified zeolite has proven to have a fixed weight after 200 °C, while the modified zeolite with APTES has shown continuous weight losses up to 500 °C. As a result, we may conclude that the TGA presents the perfect temperature for the zeolite to be used before it burns, which is from room temperature to around 200 °C. After that, the zeolite will start to lose some of its chemical bonds and structure [33].

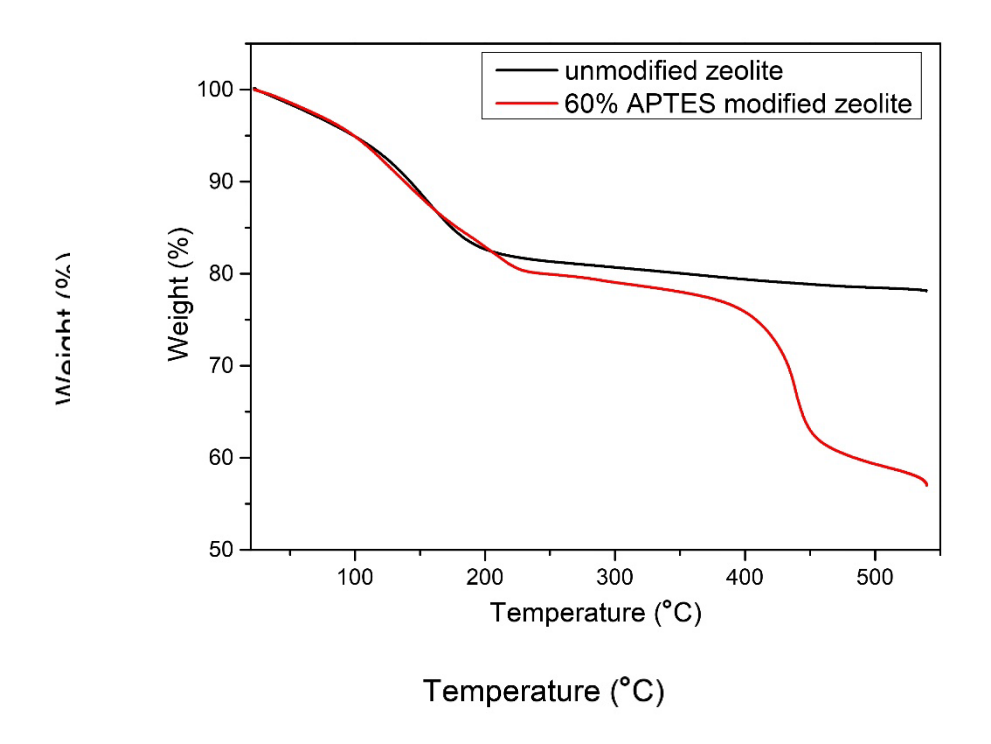


Figure 9 TGA analysis of (A) the unmodified Zeolite, and (B) Modified Zeolite with 60% APTES.

## 4. CONCLUSIONS

This study demonstrates the successful functionalization of zeolite nanomaterial with amino groups using varying concentrations of APTES, with a particular focus on enhancing its carbon dioxide adsorption performance. Among the tested concentrations, zeolite modified with 60 wt.% APTES exhibited the highest CO<sub>2</sub> adsorption capacity, exceeding 4000  $\mu$ mol/g, which represents fourfold improvement compared to the unmodified sample. This significant enhancement is attributed to the increased number of active amine sites introduced during the functionalization process, as confirmed by comprehensive characterization techniques including FTIR, XRD, FESEM, EDX, XPS, and TGA. The findings underscore the potential of amine-functionalized zeolite, especially at 60 wt.% APTES, as a highly effective material for CO<sub>2</sub> capture applications, offers a promising pathway for future development of advanced gas adsorption systems.

# Acknowledgment

This work is supported by Universiti Teknologi PETRONAS (UTP) under STIRF research grant with grant number 015LA0-085.

### References

- [1] Z. Liu, J. Zhu, C. Peng, T. Wakihara, T. Okubo, Reaction Chemistry & Engineering 4 (2019) 1699
- [2] J. Park, H. Tabata, ACS Omega 6 (2021) 21284
- [3] M. Shamzhy, M. Opanasenko, P. Concepcion, A. Martinez, Chemical Society Reviews 48 (2019) 1095
- [4] S. Lee, B. Kim, J. Kim, Journal of Materials Chemistry A 7 (2019) 2709
- [5] N. Kosinov, J. Gascon, F. Kapteijn, E.J. Hensen, Journal of Membrane Science 499 (2016) 65
- [6] Y. Hyeon, J. Lee, H. Qutaish, S.A. Han, S.H. Choi, S.W. Moon, M.-S. Park, D. Whang, J.H. Kim, Energy Storage Materials 33 (2020) 95
- [7] V. Aggarwal, S. Solanki, B.D. Malhotra, Chemical Science 66 (2022) 99
- [8] C.-H. Huang, C.-S. Tan, Aerosol and Air Quality Research 14 (2014) 480
- [9] S.A. Alnuaimi, D. Vaishnavi, H.G. Hameed, Experimental and Theoretical NANOTECHNOLOGY 9 (2025) 513
- [10] M. Anwar, M. Iftikhar, B. Khush Bakhat, N. Sohail, M. Baqar, A. Yasir, Sustainable Agriculture Reviews 37 (2020) 13
- [11] M. Filonchyk, M.P. Peterson, H. Yan, A. Gusev, L. Zhang, Y. He, S. Yang, Science of the Total Environment 944 (2024) 173895
- [12] W. Ye, W. Liang, Q. Luo, X. Liang, C. Chen, Industrial & Engineering Chemistry Research 64 (2025) 4148
- [13] C.M. Mfoumou, F. Ngoye, P. Tonda-Mikiela, F.E. Evoung, L.B. Bi-Ndong, T. Belin, S. Mignard, Journal of Environmental Protection 14 (2023) 66
- [14] M. Suba, O. Verdes, S. Borcanescu, A. Popa, Molecules 29 (2024) 3172
- [15] N. Shezad, M. Safdar, H. Arellano-Garcia, C.-W. Tai, S. Chen, D.-K. Seo, S. You, A. Vomiero, F. Akhtar, Carbon Capture Science & Technology 15 (2025) 100424
- [16] D. Madden, T. Curtin, Microporous and Mesoporous Materials 228 (2016) 310
- [17] A.A. Dabbawala, I. Ismail, B.V. Vaithilingam, K. Polychronopoulou, G. Singaravel, S. Morin, M. Berthod, Y. Al Wahedi, Microporous and Mesoporous Materials 303 (2020) 110261
- [18] J.M. Crawford, M.J. Rasmussen, W.W. McNeary, S. Halingstad, S.C. Hayden, N.S. Dutta, S.H. Pang, M.M. Yung, ACS Catalysis 14 (2024) 8541
- [19] H.N. Abdelhamid, Applied Organometallic Chemistry 36 (2022) 6753
- [20] T. Derbe, S. Temesgen, M. Bitew, Advances in Materials Science and Engineering 2021 (2021) 6637898
- [21] M. Gupta, H.F. Hawari, P. Kumar, Z.A. Burhanudin, N. Tansu, Nanomaterials 11 (2021) 623
- [22] Z. Huang, J.-F. Su, Y.-H. Guo, X.-Q. Su, L.-J. Teng, Chemical Engineering Communications 196 (2009) 969
- [23] A. Iqbal, H. Sattar, R. Haider, S. Munir, Journal of Cleaner Production 219 (2019) 258
- [24] M.J.-L. Mukaba, A.E. Ameh, C.P. Eze, L.F. Petrik, Environ. Eng. Manag. J 19 (2019) 475
- [25] R.P. Ningtyas, G. Murdikaningrum, J.M. Hutagalung, S. Kong, CHEMICA: Jurnal Teknik Kimia 11 (2024) 33
- [26] S. Soltani, A. Zamaniyan, J.T. Darian, S. Soltanali, RSC Advances 14 (2024) 5380
- [27] S. Eren, F.N. Turk, H. Arslanoglu, Environmental Science and Pollution Research 31 (2024) 41791
- [28] W.J. Roth, M. Opanasenko, M. Mazur, B. Gil, J. Cejka, T. Sasaki, Advanced Materials 36 (2024) 2307341
- [29] V. Viriya, T.L. Chew, Q.H. Ng, C.-D. Ho, Z.A. Jawad, Results in Engineering 24 (2024)

- Exp. Theo. NANOTECHNOLOGY 9 (2025) 539-553 102951
  - [30] N.B.T. Tran, N.B. Duong, N.L. Le, Journal of Chemistry 2021 (2021) 6678588
  - [31] D.C. Son, V.T.K. Anh, N.T. Thom, H.L.T. Nguyen, L.V. Hai, C.T. Thien, N.T. Hoang, T.D. Lam, P.T. Nam, N.T.T. Trang, Vietnam Journal of Chemistry 61 (2023) 170
  - [32] S.R. Bare, A. Knop-Gericke, D. Teschner, M. Havacker, R. Blume, T. Rocha, R. Schlogl, A.S. Chan, N. Blackwell, M. Charochak, Surface Science 648 (2016) 376
  - [33] P. Emayavaramban, K. Kadirvelu, N. Dharmaraj, Journal of Nanoscience and Nanotechnology 16 (2016) 9093

© 2025 The Authors. Published by LPCMA (<a href="https://etnano.com">https://etnano.com</a>). This article is an open access article distributed under the terms and conditions of the Creative Commons Attribution license (<a href="http://creativecommons.org/licenses/by/4.0/">http://creativecommons.org/licenses/by/4.0/</a>).